

# Earth's magnetic field: ocean current contributions to vertical profiles in deep oceans

F. E. M. (Ted) Lilley,<sup>1</sup> Antony White<sup>2</sup> and Graham S. Heinson<sup>3</sup>

<sup>1</sup> *Research School of Earth Sciences, Australian National University, Canberra, ACT 0200, Australia. E-mail: Ted.Lilley@anu.edu.au*

<sup>2</sup> *School of Chemistry, Physics and Earth Sciences, Flinders University, Adelaide, SA 5001, Australia. E-mail: Antony.White@flinders.edu.au*

<sup>3</sup> *Department of Geology and Geophysics, University of Adelaide, Adelaide, SA 5001, Australia. E-mail: Graham.Heinson@adelaide.edu.au*

Accepted 2001 May 24. Received 2001 May 10; in original form 2000 December 2000

## SUMMARY

The Earth's main magnetic field, arising in the core, should, in the ocean, have a well-defined uniform gradient with depth. Superimposed upon this uniform gradient may be magnetic signals due to a variety of sources. These include crustal magnetization, the transient fluctuations arising external to the Earth and causing secondary induced fields within it; and, the focus of the present paper, magnetic signals arising from the motional induction of seawater moving in the steady main magnetic field of Earth. There are circumstances where theory predicts such motionally-induced magnetic fields to be of order  $10^2$  nT, and to vary with depth in a way which is directly related to the velocity profile.

Exploratory soundings of the magnetic field with depth have been made in the oceans around Australia, both to test these predictions, and to investigate the practicability of measuring such profiles. The magnetic field parameter observed has been that of the 'total field', which should sense the component of the ocean velocity which lies in the magnetic meridian. The magnetometer has been lowered by cable from a ship and also operated free-fall to the seafloor (and return). The observations appear both to confirm the theoretical gradient of the main field where there is no ocean current and, where ocean currents exist, to give evidence of their profiles resolved in the direction of magnetic north. In particular, observations taken in an eddy of the East Australian Current show the correct contrast in sign for north and south flowing streams.

**Key words:** East Australian Current, electrical conductivity, electromagnetic induction, geomagnetism, motional induction, warm-core ring.

## 1 INTRODUCTION

Measuring the vertical gradient of the geomagnetic field has a distinctive history, connected with experiments some fifty years ago to establish the cause of the field itself. Observations were made on land, using mine shafts and one pioneering effort was made in the ocean.

Soon afterwards early 'modern' magnetometers became widely available. These instruments were based in one case on the principles of the hysteresis of iron (the 'fluxgate') and in the other case on the principles of 'proton-precession'. The latter were especially well-suited to the application, in marine geophysics, of the measurement of total-field magnetic profiles along the tracks of ships. As is well known, a far-reaching consequence of these efforts to measure horizontal profiles of the total field was the discovery of the magnetic stripes of the seafloor. This discovery in turn gave rise to plate tectonic theory.

As part of the marine applications investigated for proton-precession magnetometers in measuring crustal magnetic fields, Heirtzler (1967) used two such instruments to measure vertical gradients of the magnetic field in the Arctic Ocean. One magnetometer recorded on an ice island, and one was suspended on a cable at a depth of 305 m, as the ice island drifted laterally.

At that time also rocket-borne magnetometers measured profiles vertically above Earth's surface (Matsushita 1967). These profiles produced evidence for the existence of ionospheric electric currents, by observing the changes in magnetic field which were observed as an ionospheric current sheet was penetrated by the magnetic sensor. An early example is that of Burrows & Hall (1965).

Generally, however, little attention appears to have been paid to the measurement, which had become possible, of vertical profiles of Earth's magnetic field down through the oceans. This paper now addresses that subject. There is a fundamental

reason of geomagnetism to do so. It is to demonstrate the existence of a magnetic field which, on theoretical grounds, is predicted to be generated by ocean currents. In addition there are possible applications to oceanography, in obtaining information on the component of the ocean flow in the direction of magnetic north.

Exploratory measurements have been made off the Australian east and west coasts, especially, in the former case, where the East Australian Current (EAC) flows strongly. In the EAC, contrasting north and south flows have been intentionally measured. The purpose has been to check for the existence of signals of opposite sign, which theory predicts such opposite flows should yield. Details of the observations are given in Table 1.

## 2 HISTORY

### 2.1 Vertical profiles of Earth's magnetic field

In the late 1940's, when modern magnetometers (fluxgate and proton-precession, in sequence) were on the point of entering geophysical research with such far-reaching impact, a debate was current about the origins of Earth's main magnetic field. The debate centred on whether Earth's magnetic field was inherent in the planet as a massive rotating body, or whether it was caused by the very different process of dynamo action in Earth's core. The former case was advanced at that time by, for example, Blakett (1947), and the latter case, for example, by Bullard (1949). Runcorn *et al.* (1951) attribute to Bullard the idea that testing between these two theories was possible by measuring the vertical gradient of the strength of the field in Earth's surface layer, and this acknowledgement is confirmed by Hide (1997) in his acceptance of the William Bowie Medal of the American Geophysical Union.

The subject was widely discussed at the time, see for example Runcorn (1948) and Chapman & Runcorn (1948). Experiments on land were undertaken in both deep gold mines in South Africa (Hales & Gough 1947) and coal mines in England (Runcorn *et al.* 1951). The latter had the benefit of minimal disturbance by crustal magnetization, which affected the South African measurements. The results, as reported by Runcorn *et al.* (1951), were regarded as being 'decisive evidence against a fundamental origin of the geomagnetic field' (i.e. against the massive rotating body theory), as were, independently, the

results of the laboratory experiments of Blakett (1952). Instruments developed for the latter, now famously, opened up a new era in palaeomagnetic measurements (McElhinny & McFadden 2000).

The land-based experiments sought the vertical gradient information by observing both on the surface and at depth, in deep mines. The possibility of making 'measurements in the sea to great depth' was noted by Runcorn *et al.* (1951), with the caveat that 'induced currents due to the fluid motions might mask the effect'. One expedition, that of the Danish ship *Galathea*, is on record (Espersen *et al.* 1956) as measuring the vertical gradient of the magnetic field in the ocean, with specially constructed equipment and magnetometers based on classical principles. Notwithstanding skill in instrument design and construction, and experimental determination during the cruise, severe instrumental and logistic difficulties were encountered. Within just a matter of years, the availability of proton-precession magnetometers would change the position entirely.

### 2.2 Motional electromagnetic induction in the ocean

A second major aspect of this paper, motional electromagnetic induction, has an equally distinctive history. The commencing point is perhaps the celebrated observations of Faraday (1832) in the Thames River in London. The subject came into sharp oceanographic focus with the GEK (Geoelectrokinetograph) method for determining ocean current information, which led to the fundamental paper by Longuet-Higgins *et al.* (1954). Measurements in long telephone cables have been pursued for example by Baines & Bell (1987) and Larsen (1992), and see the review by Lanzerotti *et al.* (1993). The development of seafloor instrumentation has been led by Filloux (1987), and in the context of the present paper, seafloor electric and magnetic signals recorded by Filloux instrumentation below the East Australian Current have been the subject of the papers by Lilley *et al.* (1986), Bindoff *et al.* (1986), Bindoff (1988), and Lilley *et al.* (1993). Another relevant review is that by Palshin (1996).

A range of instrumentation for ocean-current profiling based on electric field measurements has been developed by Sanford, following theory in his paper (Sanford 1971). Aspects of the present paper are to some extent a magnetic analogue of Sanford's electric field work (Sanford *et al.* 1985).

**Table 1.** Details of the observation of vertical profiles of the total-magnetic field in the ocean column around Australia, 1994–1997. The site positions relevant to the present paper are listed in Table 2. The agreement between the IGRF gradients for the Indian Ocean (site 4) and the Tasman Sea is coincidental.

Year of observation	1994	1995	1997
Area	Tasman Sea	Indian Ocean	Tasman Sea
Style of cast	(a), from ship	(b), from ship	(b); (c)
Number of casts	1	14	7; 2
Type of magnetometer	Overhauser	Overhauser	Proton-precession
Base station control	Canberra	Learmonth	land & seafloor
Surface floater control	no	no	yes
Depth of ocean (m)	5000	1800	5000
Depth of cast (m)	3400	1800	5000
IGRF gradient pT m <sup>-1</sup>	-29.7	-29.7	-29.7

Global-scale treatments of motional electromagnetic induction in the ocean include the calculations of Stephenson & Bryan (1992), with attention to the external magnetic field (which is zero in the model adopted for the present case). There are further theoretical treatments by Chave & Luther (1990) and Luther *et al.* (1991), and other relevant recent papers are those by Chave *et al.* (1997), Flosadottir *et al.* (1997a, 1997b), Tyler *et al.* (1997) and Fujii & Chave (1999). The contribution by Runcorn and Winch in Barraclough *et al.* (1992) deals with evidence for an annual signal generated by ocean currents in the geomagnetic field.

In many of the above papers, emphasis is on observation of the electric field, which has traditionally been experimentally easier to measure. The present paper however emphasizes magnetic observations, both as a prime concern of geomagnetic research, and because modern magnetometers open up new possibilities of marine magnetic field measurement. Recently Toh *et al.* (1998) reported vertical profiles of total field recorded in the Sea of Japan.

### 3 THEORY

#### 3.1 The main geomagnetic field

It is elementary to show that for a spherical earth of radius  $R$ , with a magnetic field due to a central axial dipole of strength  $m$ , all magnetic field components (horizontal, vertical and total) fall off as  $r^{-3}$  where  $r$  denotes radial distance from the centre. In particular if a model for the Earth is taken with radius 6371 km and central dipole strength  $8 \times 10^{22}$  A m<sup>2</sup> (Merrill *et al.* 1996), then the total-field at the surface will have a vertical gradient of  $-20$  pT m<sup>-1</sup> (i.e.  $-20$  nT m<sup>-1</sup>) at the equator, changing with latitude to  $-40$  pT m<sup>-1</sup> at the poles. These values give a useful guide to what may be expected at the Earth's surface. Although the total-field strength is inversely proportional to the third power of radial distance, because measurements even in a deep ocean (of depth say 5000 m) involve only a small change in radius from Earth's centre, the radial (or, as it is seen, vertical) gradient may be expected to be effectively uniform over the ocean column for practical purposes.

Modern values for the International Geomagnetic Reference Field (IGRF) allow straightforward determinations of the actual vertical gradients to be expected for the real Earth. For the positions where the observations of this paper were made, values of the vertical gradient have been computed from the IGRF values of Barton (1997). These values are listed in Table 1.

#### 3.2 The motionally induced magnetic field

This section draws upon the paper by Sanford (1971), following the work of Longuet-Higgins *et al.* (1954). The notation adopted follows Lilley *et al.* (1993).

The physical circumstances are as in Fig. 1. The seawater has electrical conductivity  $\sigma_1$ , and is underlain by a sedimentary layer of conductivity  $\sigma_2$ , below which the conductivity is taken as zero. The ocean velocity is in the  $y$  direction, and varies with  $z$  only. Denoting the ocean velocity  $v_y(z)$  by  $v(z)$ , the electric

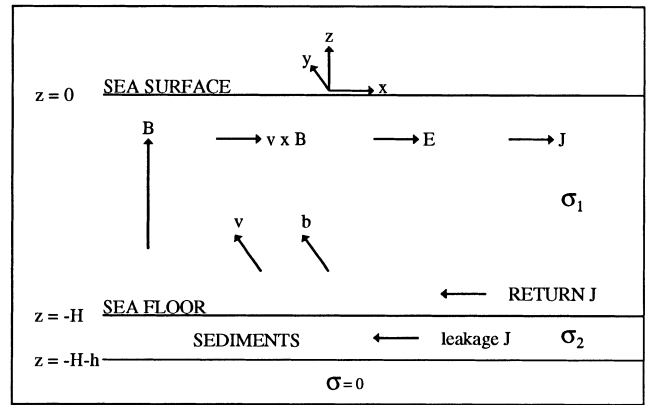


Figure 1. Figure for theory of motional induction.

current flow  $J_x(z)$  by  $J(z)$ , the electric field  $E_x$  by  $E$ , the steady vertical magnetic field  $B_z$  by  $B$ , the perturbation magnetic field  $b_y(z)$  due to motional induction by  $b(z)$ , and the local electrical conductivity by  $\sigma(z)$ , then Ohm's law for a moving medium may be expressed

$$J(z) = \sigma(z) \{ E + v(z)B \}. \quad (1)$$

The horizontal electric field  $E$  is constant from sea surface to seafloor and there is variation of the horizontal electric current  $J(z)$  with depth, corresponding to the variation with depth of velocity  $v(z)$ . For the purposes of this section, the gradients of  $B$  horizontally and vertically (as in section 3.1) are ignored.

The perturbation field  $b(z)$  due to motional induction is directly expressed as:

$$b(z) = \frac{1}{2} \mu_0 \left\{ - \int_{-H-h}^z J(z) dz + \int_z^0 J(z) dz \right\} \quad (2)$$

for  $z$  in the range  $-H-h < z < 0$  (and outside this range  $b(z)$  is zero). The first term in eq. (2) represents electric current sheets flowing below the level of measurement, and the second term represents electric current sheets flowing above that level. Eq. (2) may be written

$$b(z) = \frac{1}{2} \mu_0 \left\{ - \int_{-H-h}^0 J(z) dz + 2 \int_z^0 J(z) dz \right\}, \quad (3)$$

which, differentiating with respect to  $z$  and substituting from eq. (1) gives

$$\frac{db(z)}{dz} = -\mu_0 \sigma(z) \{ E + v(z)B \} \quad (4)$$

and

$$v(z) = -\frac{E}{B} - \frac{1}{\mu_0 \sigma(z) B} \frac{db(z)}{dz}. \quad (5)$$

Adopting notation  $\bar{v}^*$  for the constant quantity  $(-E/B)$ , making the approximation that the seawater is of uniform conductivity  $\sigma_1$  as shown in Fig. 1, and introducing notation  $\eta$  as

$$\eta = -\frac{1}{\mu_0 \sigma_1 B}, \quad (6)$$

allows eq. (5) to be written

$$v(z) = \bar{v}^* + v_s(z), \quad (7)$$

where the depth-dependent component of the velocity,  $v_s(z)$ , has been introduced as

$$v_s(z) = \eta \frac{db(z)}{dz}. \quad (8)$$

This quantity,  $v_s(z)$ , will be evaluated from the gradient (or ‘local slope’) of observed magnetic profiles presented below.

The notation  $\overline{v^*}$  used for  $(-E/B)$  is Sanford’s vertically-averaged and sea water conductivity-weighted water velocity. Its significance may be demonstrated by integrating eq. (1) over the total column of ocean plus seafloor sediments, when variation of conductivity with depth is allowed, i.e.:

$$0 = E \int_{-H-h}^0 \sigma(z) dz + B \int_{-H}^0 \sigma(z) v(z) dz, \quad (9)$$

where the left-hand side is zero due to the requirement of return electric current balance in the vertical plane. Thus

$$E/B = - \int_{-H}^0 \sigma(z) v(z) dz / \int_{-H-h}^0 \sigma(z) dz \quad (10)$$

and the quantity  $\overline{v^*}$ , multiplied by the depth of the water column, gives an estimate of the barotropic transport of the ocean current.

The quantity  $v_s(z)$  introduced in eq. (7) is the baroclinic velocity of oceanography, and will be referred to as such below. Other aspects of this theory are discussed in Lilley *et al.* (1993), where there is a ‘worked example’ illustrating some characteristics of motional induction.

### 3.3 Recovering ocean current information from observed total-field magnetic profile data

With reference to Fig. 1 the horizontal direction of  $v$  is general, and so also is the horizontal direction of  $b$ , which is parallel to  $v$ . The complete profiling of  $b$  vertically through the ocean column would thus require measurement of both its direction and strength. This task is made difficult by the lack of a reference direction, because the use of a magnetic compass, which is common in marine instruments, is not possible when measuring changes in the magnetic field itself.

However a total field magnetometer, with no particular orientation, senses the component of a perturbation field which is parallel to the dominating, main geomagnetic field. It is this principle which now allows the observation of the component of  $b$  parallel to the main field. The observed component will be  $b_n(z) \cos I$ , where  $b_n(z)$  is the component of  $b$  in the (horizontal) direction of magnetic north, and  $I$  is the inclination of Earth’s magnetic field.

Note that a total field magnetometer does not sense small field changes which are perpendicular to the main field, i.e. in the east–west direction. Thus also, no information is obtained about the component of ocean current in the magnetic east–west direction.

Eq. (8) can therefore be applied to measured total-field data, to give a profile with depth of the magnetic north component of the baroclinic ocean current. The  $\cos I$  factor introduced above is one of attenuation, and to recover  $b_n(z)$  from measurements of total-field an amplifying factor is needed, notably  $\sec I$ . If the total-field signal due to motional induction is  $f(z)$  in a general

total-field signal of  $F(z)$ , the relation is

$$b_n(z) = f(z) \sec I. \quad (11)$$

Denoting by  $v_n(z)$  the component of the baroclinic velocity in the direction of magnetic north, eq. (8) becomes

$$v_n(z) = \eta_F \frac{dF(z)}{dz}, \quad (12)$$

where

$$\eta_F = - \frac{\sec I}{\mu_0 \sigma_1 B}, \quad (13)$$

and where now  $dF(z)/dz$  will also include, as an effectively constant value, the radial or vertical variation of Earth’s main magnetic field, originating in the core.

The baroclinic velocity profile is thus relative and needs to have its baseline set by clamping to a known value at some level. The seafloor is one place where  $v(z)$  may be expected to be zero, but in the present paper  $v(z)$  is set to zero half-way down through the ocean column, to avoid effects of seafloor magnetization having a disproportionate effect.

Note that in an ideal case with no seafloor magnetization effects, the value of the baroclinic component  $v_n(z)$  at the seafloor will be the magnetic north component of  $-\overline{v^*}$ ; plus a contribution due to the gradient of the core field. By determining the former and making an estimate of the latter, a value is thus obtained of the magnetic north component of the barotropic current in the ocean column.

### 3.4 Magnetic field of magnetized crust

The anomalies of the seafloor-spreading stripes have amplitudes at the sea-surface of order  $10^2$  nT, so it is clear they will be greater at the seafloor, and that generally the crustal magnetization patterns of the seafloor will also contribute a gradient to vertical profiles observed in the ocean column.

It is planned to give this topic more attention in future measurements, and aspects of such a strategy are discussed in Section 6 below. The examples of the present paper are not well-controlled in this way, but for the most part have benefitted from the situation in the Tasman Sea that on the seafloor lies 1 km of weakly magnetized sediment, which will have an attenuating effect on the magnetic patterns of basalt underlying it.

There is also the circumstance that in an ideal case where seawater movement is restricted to the upper part of the water column, in the lower part of the water column the magnetic gradient caused by motional induction will be uniform. In eq. (7) the situation is  $v_s(z) = -\overline{v^*}$ , a constant, for  $v(z) = 0$ . As crustal magnetization will affect mainly the lower part of the profile, any strong effects it has there should be obvious.

Regarding the profiles reported in this paper, for the 1994 sounding in the Tasman Sea the magnetometer stopped 1600 m above the seafloor, and no seafloor magnetization effects were detected. Similarly the uniform gradient in the 1995 profile for the Indian Ocean (site 4) is consistent with seafloor magnetization having negligible effect.

For the 1997 soundings in the Tasman Sea, all sites except the most eastward show profiles in the lower part of the ocean which indicate that crustal magnetization has only a minor effect. The most eastward (sites 1 and 7), however, show gradients

which increase near the seafloor. This behaviour is most directly attributed to seafloor magnetization, and possibly these sites are near a volcanic extrusion on the seafloor. To some extent such effects, spurious in the present context of motional induction, are mitigated by the procedure which has been adopted, of clamping the velocity profile to zero at depth 2500 m. For sites 1 and 7, velocity information below 2500 m should be disregarded.

There is also the question of seafloor debris, dropped from passing ships. Some 1997 soundings were made in the main shipping corridor between the two major ports of Melbourne and Sydney and debris on the seafloor is thought to be the explanation of some minor effects close to the seafloor in one profile (the free-fall profile at site 6).

The magnetic effects of the ship in the upper 300 m of the water column are always present in lowered profiles. This part of the profile is important, and one main purpose for developing free-fall (and return) equipment has been to avoid the effects of a ship's magnetic field.

### 3.5 Magnetic fields of the daily variation and magnetic storms

Earth's magnetic field changes on time scales of days and shorter, due to primary changing fields which originate external to Earth and to secondary fields which are induced in the conducting Earth (and its oceans). A daily variation is generally present, and Hitchman *et al.* (1998) give total-field curves for a global model of the daily variation, as a function of latitude and local time.

In the present paper each profile has been measured over as short a time space as possible, to minimize the field changes with time during it. Also, the field has been monitored at fixed stations (either on nearby land or seafloor). Reference to the fixed-station data gives confidence that no major transient fluctuations occurred while significant profiling measurements were taking place. Also most of the measurements were intentionally carried out at night, when the daily variation is known to be generally at a minimum.

More detailed reduction for time-changes is clearly possible, but is not included here.

## 4 APPARATUS

The central part of the apparatus developed has been an appropriate package for a recording total-field magnetometer, of the type commonly used for ground magnetometer surveys in exploration geophysics. Both proton-precession and Overhauser instruments have given good results. The principles of recording the 'total-field' lead to information on the component of ocean current in the direction of magnetic north.

In the first version, shown in Fig. 2(a), both detector head and magnetometer console, set to operate in 'observatory' mode with readings every 15 s, were packaged together, with an auxiliary battery, in a glass sphere of diameter 17 in (0.43 m). The 1994 Tasman Sea data were recorded with this arrangement, which was lowered from a ship with a rope link 40 m long between the end of the ship's steel cable, and the instrument.

The detector head was found to be affected by a signal of some 10 nT from its recording console, and the next development (Fig. 2b) put detector head and console 1.8 m apart, in separate spheres of diameter 10 in (0.25 m) and 17 in (0.43 m)

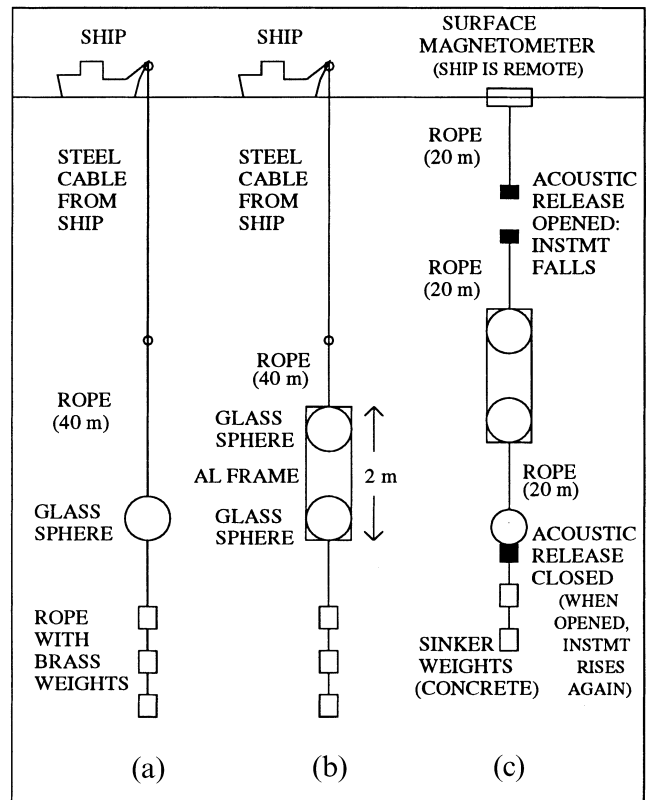


Figure 2. Sketch diagram of equipment developed for vertical magnetic profiling. (Note gross changes of scale in different parts of the figure.)

respectively. The two spheres were held by an aluminium frame, and electrically connected by appropriate marine cables. The 1995 data were observed with this arrangement. The noise was much reduced, though still greater than optimum (due to the presence of a steel washer in the detector head sphere, found and removed at the end of 1995).

The next version of the instrument, Fig. 2(c), operates in 'free-fall' mode. It is left remote, when at and near the surface, from the magnetic effects of the ship, which has moved away. The 1997 data were collected using first the apparatus of Fig. 2(b) and then using that of Fig. 2(c).

In the presentation of the results which follow, all profiling data were recorded at intervals of 15 s. These time series have been converted to depths and are presented as such, on the basis of cable out, which was logged separately with time. For the free-fall data, uniform rates of ascent and descent have been assumed in all cases.

Reference stationary magnetometers monitoring the changes of the magnetic field with time have been an important part of the profiling observations, and these are summarized in Table 1. The 1997 experiment included using the floating magnetometer (uppermost in arrangement c in Fig. 2) as a monitor of magnetic fluctuations at the ocean surface. Later (in 1998, off southern Australia) this apparatus was intentionally left floating free in the open ocean to record the magnetic signals generated by ocean swells and also to determine surface induction arrows by using also land reference data. These 1998 experiments (part of a larger SWAGGIE experiment) are reported in Hitchman *et al.* (2000).

In a wider description of apparatus the RV Franklin and its collective equipment, including especially Acoustic Doppler

**Table 2.** Geographic positions of vertical total-field magnetic profiles referred to in this paper.

Year	Cruise code	Site number	Latitude (°S)	Longitude (°E)
1994	Fr04/94	1	36.176	151.170
1995	Fr04/95	4	28.260	112.518
1997	Fr08/97	1	36.314	152.216
1997	Fr08/97	2	36.307	151.816
1997	Fr08/97	3	36.244	151.422
1997	Fr08/97	4	36.242	150.973
1997	Fr08/97	5	36.104	150.828
1997	Fr08/97	6	36.348	150.616
1997	Fr08/97	7	36.420	152.157

Current Profiler (ADCP) equipment should also be included. The ship's ADCP data are included in the examples, as is one satellite image.

## 5 RESULTS

### 5.1 Sites

The observation sites are shown in Fig. 3, and correspond to the different stages in the development of the equipment. Stage (a) of the equipment was tested in the East Australian Current in 1994 (cruise Fr04/94). Stage (b) of the equipment was tested in the Indian Ocean in 1995 (cruise Fr04/95). Stage (b) was put into production, and stage (c) tested, during 1997 in the East Australian Current (cruise Fr08/97). The geographic positions of profiles referred to in this paper are listed in Table 2.

### 5.2 Data reduction

The ensemble of observations upon which the main results of this paper are based comprise magnetic data as time series from the profiling apparatus as described in Section 4, ADCP data from the ship's fitted equipment, satellite images of sea-surface temperature which indicate surface currents, and magnetic data as time series from a variety of installations, which monitored

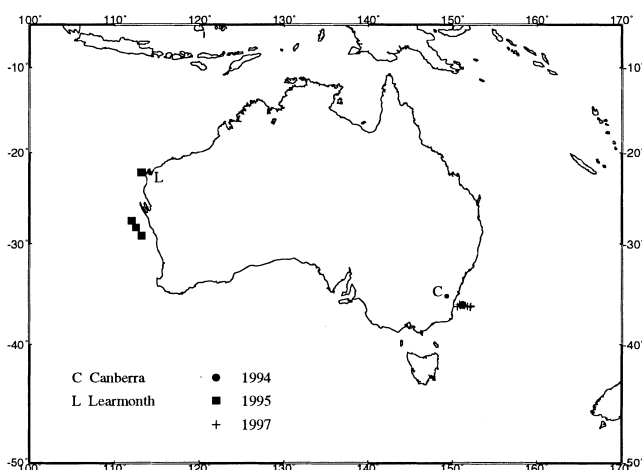


**Figure 3.** Map of Australia showing the sites referred to in the present paper.

magnetic field changes during profiler measurements, and so give 'base-station' information. Some general procedures have been followed, which it is appropriate to summarize here.

Data from magnetic profiler downcasts are taken in preference to data from upcasts, as the instrument package in downcasts is believed to travel more nearly vertically through the ocean column. By the time an upcast starts, the ship at the surface has commonly moved laterally relative to the instrument package on the end of the cable near the seafloor, causing horizontal translation of the instrument package during the upcast.

The equipment was not fitted with a recording pressure meter (the standard oceanographic method to determine depth) and winch readings of the amount of cable paid out are taken to give depths of the equipment at the end of the cable (adding also the length of any rope used there to isolate the equipment from the cable's magnetic effects).

The data as observed during a downcast were typically smoothed by the application of a nine-point running median filter.

Ship's magnetic effects are taken to be generally negligible at depths of 400 m and more below the vessel. There is a variety of evidence in the data of the present paper which supports this limit.

### 5.3 Tasman Sea, April 1994

With the prototype magnetometer package as described, a single cast was made into the Tasman Sea from the RV Franklin in April 1994. A site was chosen on the basis of satellite images, where the surface current was indicated to be flowing strongly southwards. The observation site is shown Fig. 3. The length of cable available allowed a cast of some 3400 m into water of depth 5000 m. The data obtained are shown in Fig. 4. These are basically raw data and while they have the imperfections of noise (basically magnetic contamination) they nevertheless are considered to show, qualitatively, the characteristics sought. The downcast first shows the effects of the ship's magnetic field, but once these are out of range (at ordinate reading 12 hours), it is clear that the profile with depth is curved, notwithstanding the presence of the oscillating signal attributed to slowly rotating apparatus and minor magnetic contamination. Fig. 4 also shows the record for the same time from Canberra Magnetic Observatory. It can be seen that the downcast was made during quiet magnetic conditions.

### 5.4 Indian Ocean, April–May 1995

The next version of the instrument, described in Fig. 2(b), was tested from the RV Franklin in the Indian Ocean in 1995, in a cruise of opportunity. Satellite images, checked for activity in the Leeuwin Current which flows off the West Australian coast, showed that little current was present where the casts were made. In addition to testing the equipment, the observations thus become useful as a test of background effects, and, in particular, as test measurements of the uniform gradient which should characterize the main geomagnetic field in the ocean.

A total of 14 casts were made, at sites shown in Fig. 3. An example of these results is included here particularly to show how, with little ocean current, the observed gradients do follow the expected theory of a uniform gradient for Earth's main

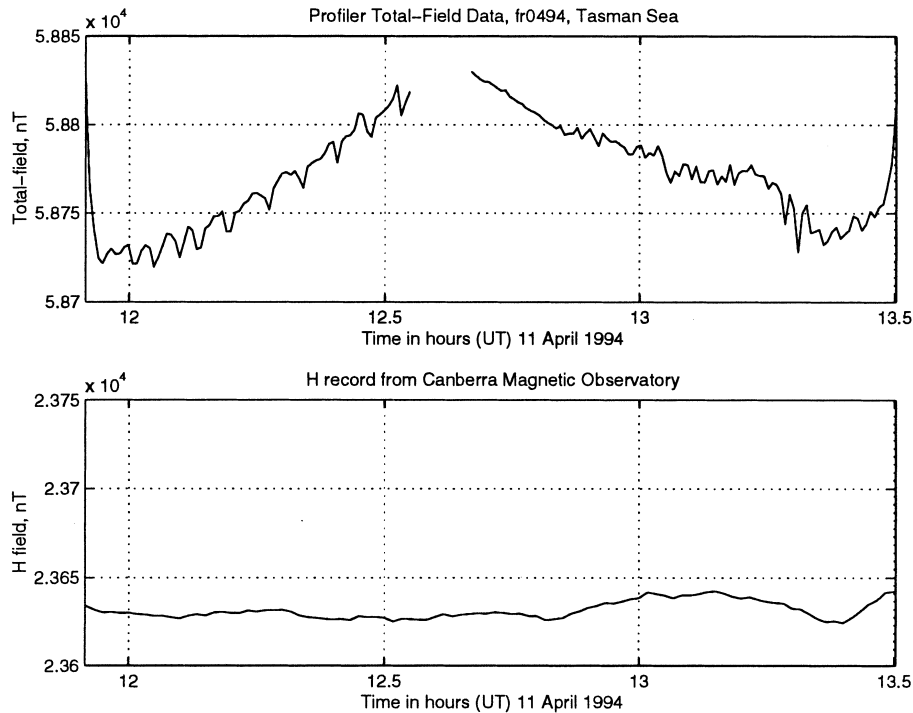


**Figure 4.** Profiler (total-field) and Canberra Observatory (H-component) data, April 1994, Tasman Sea. The cast is to depth 3400 m in water 5000 m deep. The downcast is considered to be more nearly vertical through the water than the upcast. Also, in this instance, the observatory data show the downcast to have taken place during a time of more constant magnetic field than the upcast. The 'sinusoidal' signal which is present in the downcast is thought to be due to magnetic contamination (not removed at that stage) in the magnetometer package, which is rotating slowly as it descends. On the upcast, the forces on the magnetometer package are quite different, and its behaviour is quite different. There is no evidence of the slow rotation. Instead, for the first quarter of the upcast, the magnetometer record is good, before instrument performance deteriorates and the record becomes noisy, due possibly to the whole package vibrating as it is hauled up through the ocean column.

field in the deep ocean. The results thus serve as a benchmark against which profiles observed in an ocean current may be judged.

The basic observed data obtained for the two casts at site 4 are shown in Fig. 5. As can be seen, a uniform gradient is observed, better displayed in Fig. 6 where the data of the second downcast is re-plotted, having been filtered and corrected for variations in winch speed (which typically occur, for mechanical reasons, near the start and finish of any particular downcast or upcast). The magnetic influence of the ship can be seen to extend to a depth of some 300 m beneath it.

The figure also shows the gradient predicted for the site by the IGRF, arbitrarily drawn through the origin of the figure. The observed gradient is slightly stronger than that of the IGRF, indicating presumably the effects of shorter-wavelength crustal magnetization than are included in the IGRF model. Also, the absolute surface value predicted by the IGRF is 56924 nT, some 80 nT greater than observed. These discrepancies with the IGRF, of gradient and surface value, are not regarded as serious.

### 5.5 Tasman Sea, September–October 1997

The observations of 1997, part of the Study of Ocean Dynamo Action (SODA) experiment, comprised a main objective of a 10 day cruise of RV Franklin. The ship was free to go to places where strong north- and south-flowing currents might be found. A large eddy, or warm core ring, was chosen, on the basis of satellite images, one of which is shown in Fig. 7. This feature

was sitting south of latitude 35°S, where the East Australian Current leaves the Australian coast (Cresswell & Legeckis 1986; Tomczak & Godfrey 1994).

The general velocity characteristics of this eddy as deduced from the satellite images were confirmed by the ship during the cruise and a compilation of all ADCP data during the cruise is shown in Fig. 8.

The sites of the vertical profiling are also marked on Fig. 8. After a traverse across the eddy from west to east, deploying seafloor magnetometers and making oceanographic observations, the eddy was then traversed from east to west, with vertical profiling carried out from the ship at sites 1 to 5. Two 'free-fall' profiling operations were then carried out at sites 6 and 7, one on each side of the eddy. Bad weather prevented more free-fall profiles in the ship-time available. There are thus seven profiling sites for the eddy.

### 5.6 Profiles, lowering instrument from ship

The observed data from the ship casts are not dissimilar to those presented in Fig. 4, (but without the contamination signal evident there, which by 1997 had been removed). Such observed data are not presented again, but instead the data from all five sites are presented first as profiles of vertical magnetic gradient, and then as profiles of the magnetic north component of baroclinic velocity.

The values of vertical gradient have been computed quite directly from the basic profiler observations, after the latter were passed through a simple median filter. The gradient

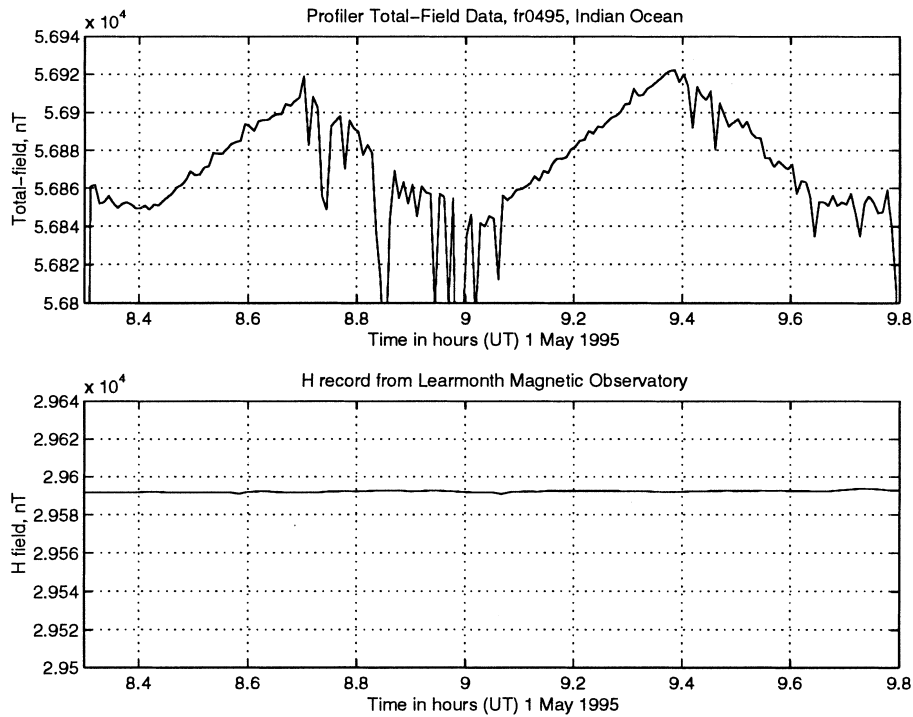


**Figure 5.** Profiler (total-field) and Learmonth Observatory (H-component) data, May 1995, Indian Ocean, site 4. The casts are to near-bottom, in water 1800 m deep. The major sections of the record evident are, in order: downcast, upcast, downcast, upcast. Note wind speed varies at the start and finish of each cast. As for the upcast in Fig. 4, the noise spikes recorded during the upcasts are attributed to degraded magnetometer performance, possibly caused by vibration.

estimates are also smoothed, again in a simple manner, by taking the mean gradient over typically 100 m of profile. The vertical gradient profiles thus obtained across the eddy are presented in Fig. 9.

Profiles of the magnetic north component of baroclinic velocity have been computed, by application of eq. (12), from the data in Fig. 9. Adopting, for the Tasman Sea data, numerical values of  $\mu_0 = 4\pi \times 10^{-7}$  H/m,  $\sigma_1 = 3.3$  S/m,  $I = -66.7^\circ$ , and

$B_z = 54000$  nT, gives

$$\eta_F = -11.3 \text{ m}^2 \text{ s}^{-1} \text{ nT}^{-1}. \quad (14)$$

The profiles thus obtained for the north component of baroclinic current across the eddy are shown in Fig. 10.

In this application of eq. (12), it is helpful to think of  $\eta_F$  as  $-0.0113 \text{ m s}^{-1}$  per  $\text{pT m}^{-1}$ , so that a negative gradient (a decrease outwards or upwards, in the sense of Fig. 1) of the total magnetic field of  $10 \text{ pT m}^{-1}$  corresponds to an estimate for the magnetic north component of the baroclinic ocean current of  $0.113 \text{ m s}^{-1}$ .

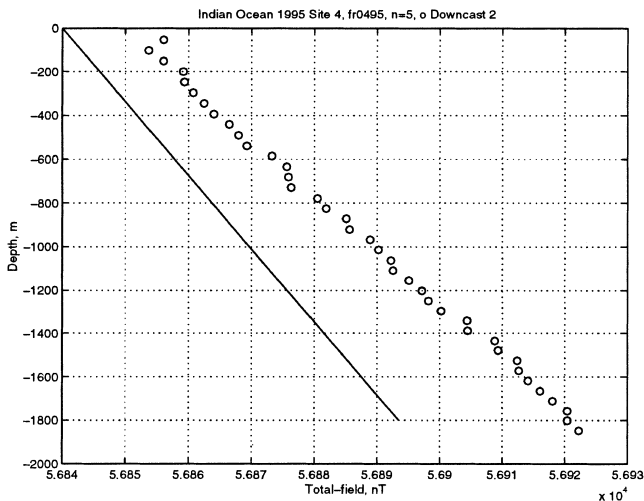


**Figure 6.** Downcast data from Indian Ocean site 4, median-filtered, and corrected for wind speed. Also shown is a line with the gradient predicted for the site by the IGRF. The actual surface value predicted by the IGRF is 56924 nT, which can be seen to be some 80 nT greater than observed. The magnetic effects of the ship in the upper 300 m of the cast are evident.

### 5.7 Profiles, ‘free-fall’

The two ‘free-fall’ (and return) casts achieved during the 1997 SODA experiment, though regarded as developmental at the time, have yielded crucial observations. Their importance lies particularly in the attainment of their prime objective, to avoid the magnetic effects of the ship and give profiles from the surface down. A characteristic of the East Australian Current is that its greatest velocity shear is within several hundred metres of the ocean surface. It is just at these depths that, for ship casts, the ship’s magnetic effects spoil the profiler data. The ‘free-fall’ equipment was developed to avoid this problem. It was first tested at the end of the ship-cast operations, due to the hazard of loss in such tests (fortunately not realized).

The two free-fall profiles are therefore now discussed separately from the grouping above of the casts from the ship at the sites 1 to 5. The data obtained are presented in Fig. 11, both as profiles of the vertical magnetic gradient, and as profiles of the magnetic north component of the baroclinic current.

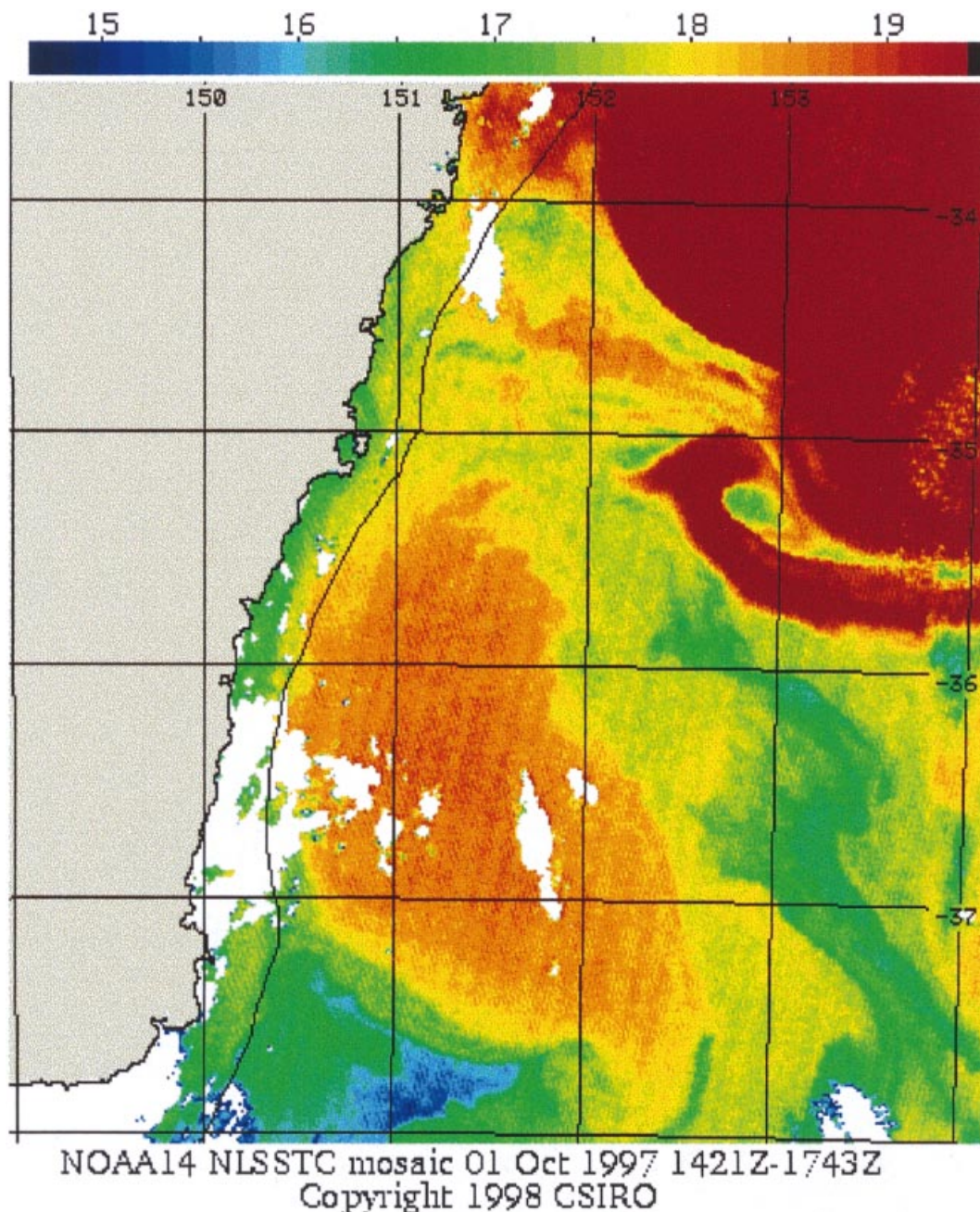


**Figure 7.** A satellite image of the warm-core ring in the East Australian Current, 1 October 1997. The scale at the top of the figure gives sea surface temperature in °C. The line of profiling sites crosses the eddy south of the 36° parallel of latitude (see Fig. 8)

Data from the nearest regular ship-cast sites are included for comparison. In the case of free-fall site 6, ship-cast site 5 was made just two days earlier, but at a significantly different site; site 5 is in deep ocean (depth 5000 m.) while, due to ship logistics in bad weather, site 6 is half way up the continental shelf (depth 2500 m.) Free-fall site 7, however, is virtually at the same site as ship-cast site 1, but was five days later.

Inspection of Fig. 11 shows a great deal of pleasing consistency, between ship-casts and free-fall casts in similar ocean current situations. Thus, for sites 1 and 7, the plots for site 7 overlie the plots for site 1 (for which there were two downcasts, a matter of hours apart). Especially pleasing is the way in which the strong shear profile is now carried smoothly all the way to the surface.

Similarly for sites 5 and 6, although there is an offset in vertical gradient 'zero level', which gives an offset in baroclinic velocity, it is again pleasing to see that the shape of the profiles is very similar. Again the strong velocity shear near the surface suggested by the ship cast is confirmed, and carried right to the surface, by the free-fall cast.

## 6 DISCUSSION

### 6.1 Profiles of the component of ocean current in the magnetic meridian

In Fig. 12, various sets of data are brought together. First the ship-cast profiles from Fig. 10 are plotted, with each given the

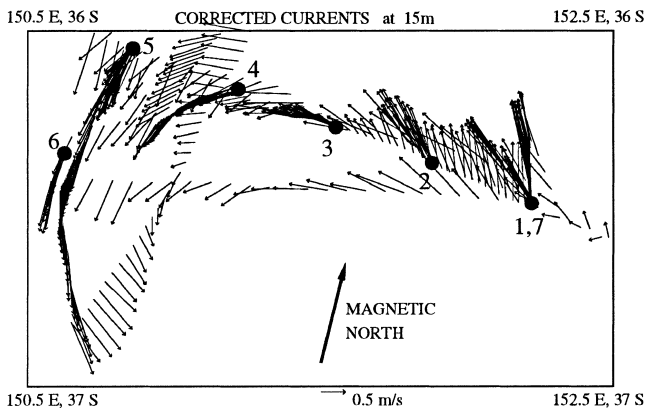


**Figure 8.** Ship's ADCP information on surface currents for the warm-core ring in the East Australian Current, cruise Fr08/97, September–October 1997. The numbers refer to the profiling sites in Table 2. The magnetic declination for the area is  $13.7^\circ\text{E}$ .

appropriate base-line shift to make it zero at depth 2500 m. To the ship-cast data for site 1 are then added, from Fig. 11, the free-fall data for site 7, to give profiles all the way to the sea surface. These profiles are also clamped to zero at depth 2500 m. Finally, the profiles obtained from the ship's ADCP equipment are added; these typically extend just several hundred metres down from the sea surface, and so contribute to filling the gap (caused by the ship's magnetic field) in the upper 400 m of the ship-cast data.

As a test of the method, the combined profiles for sites 1 and 7 in Fig. 12 are particularly significant. There is consistency in the upper 500 m of the water column between the free-fall profile data, and the ADCP data. Below 500 m there is consistency between the free-fall data and the ship-cast data. The free-fall data for site 7 thus give confidence, at other sites, in interpolating between the ship-cast data and the ADCP data.

The picture as evident in Fig. 12 is then generally consistent with what is understood of a warm-core ring in the East Australian Current. In particular the strong currents, of strength

order  $1\text{ m s}^{-1}$  at the surface, decay with depth to be effectively zero at depth 1500 m. Because the coastline of east Australia strikes approximately magnetic north-south, the component of current in the magnetic meridian as shown in Fig. 12 is the along-shore component, and indicates transport in this part of the Tasman Sea parallel to the coastline.

## 6.2 Measuring the vertical component

In the light of the experience gathered in the development and use of the profiling magnetometers, some further refinements in the method come immediately to mind. For example, it is straight-forward conceptually to add to a profiling magnetometer another magnetic sensor to measure the vertical component of the magnetic field. A fluxgate sensor, set on gimbals, might achieve this objective well. Data from such a sensor could be used to check the assumption in eq. (11) that the signals measured are indeed the resolved component of a signal which was originally horizontal.

Vertical-field data may also help resolve crustal magnetic field contributions, and give warning of other stray magnetic effects.

## 6.3 Gradiometer measurements

Pairs of proton-precession magnetometers lend themselves to operation in gradiometer configurations, and vertical gradiometer profiles in the ocean may have the advantage of being minimally affected by time-fluctuations of the ambient magnetic field. This benefit is a major reason for the use of gradiometer signals in other magnetic mapping applications.

In the ocean context there is a great freedom in designing the distance between the two sensors of a gradiometer apparatus, over which the vertical gradient is measured. Optimizing this distance may be an important task, as there may be a trade off between the accuracy of the gradient measurement, and the finest scale of magnetic signal (and ocean movement) which can be detected.

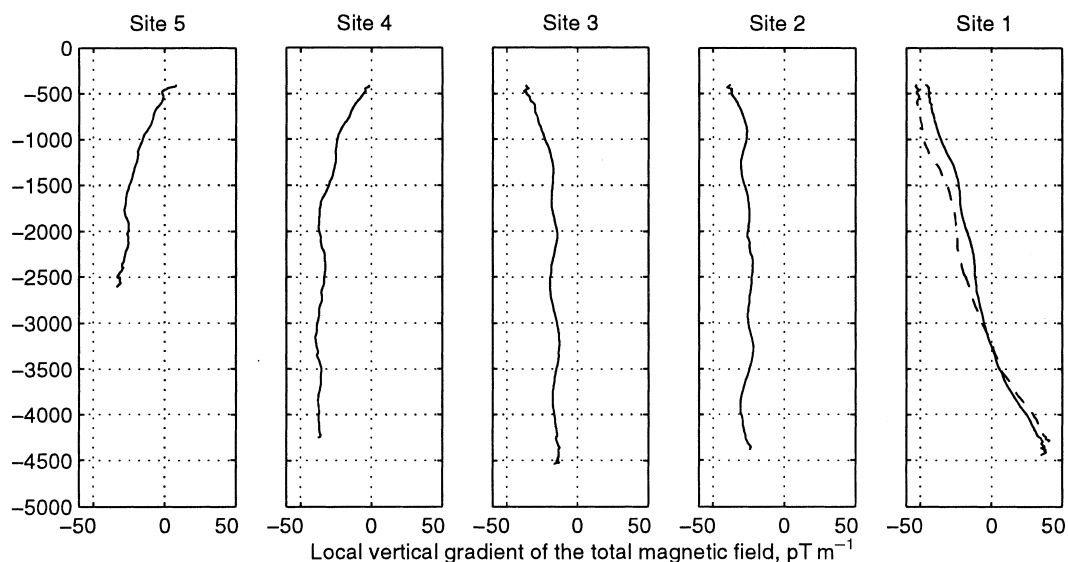


**Figure 9.** Downcast data from sites 1 to 5, median-filtered, corrected for wind speed, and reduced to give profiles of the vertical gradient of the total magnetic field. The ordinate of the plots is depth in m. The dashed line at site 1 indicates a second cast there, approximately 2.5 hr after the first cast.

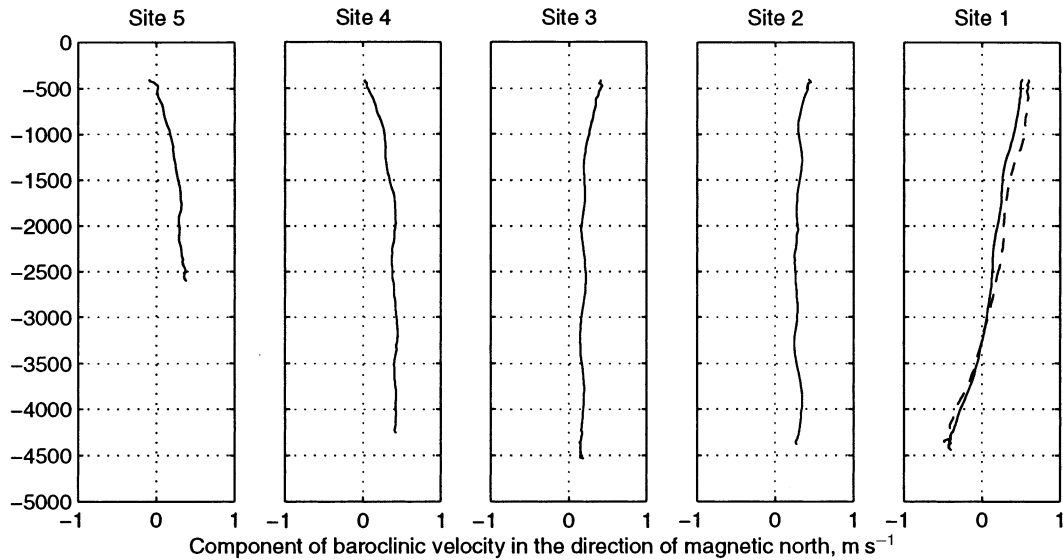


**Figure 10.** Downcast data from sites 1 to 5, median-filtered, corrected for winch speed, and reduced to give profiles of the component of baroclinic velocity in the direction of magnetic north. Each such profile needs a zero shift to convert it to actual velocity, and such zero shifts are shown carried out in Fig. 12. The lower half of the profiles for site 1 are considered to be influenced by seafloor magnetization effects and should be ignored from an oceanographic point of view.

#### 6.4 Magnetic maps of ocean areas

To further control the question of crustal magnetization effects, vertical profiles may be sought where suitable magnetic maps of an ocean area are held. For an area such as that studied in the

1997 SODA experiment, it may be rewarding to compile a surface magnetic map for the specific purpose of controlling crustal magnetization effects in vertical profile data. Due to its position in a western boundary current, strong oceanographic features are often present in the 1997 SODA region, which is

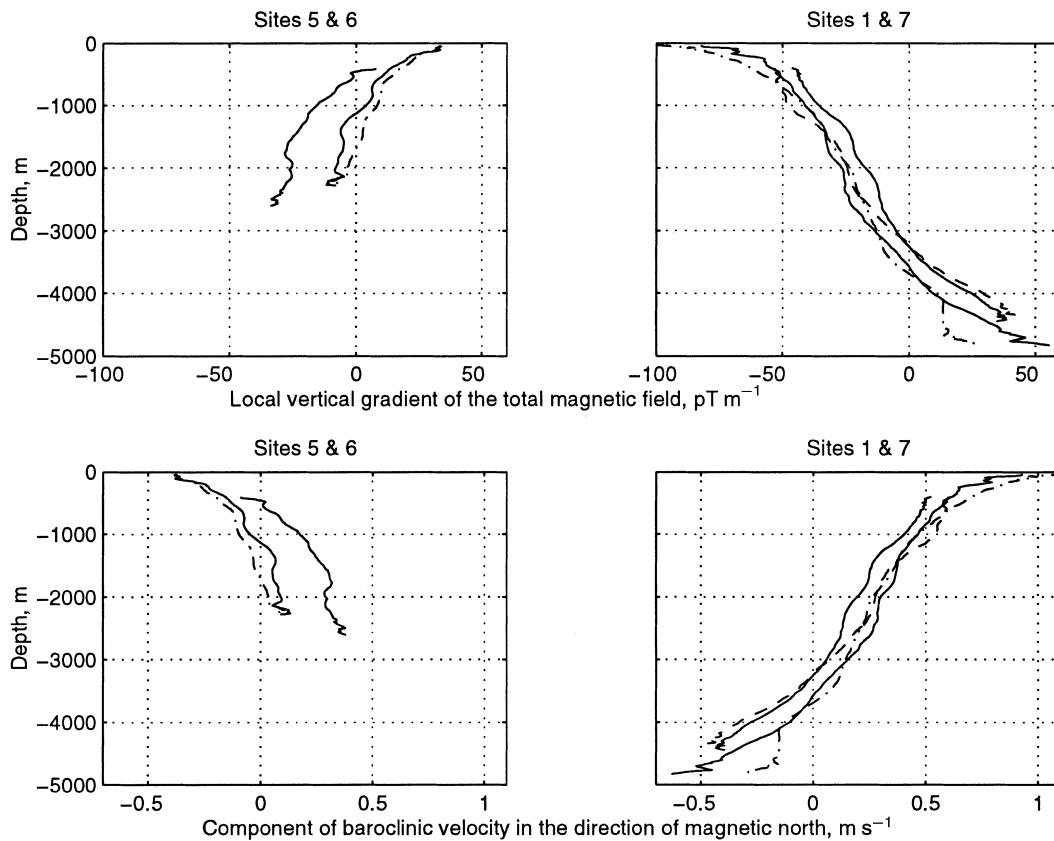


**Figure 11.** Results obtained by free-fall casts at sites 6 and 7, plotted with results obtained by ship casts at sites 5 and 1, respectively. Where the profiles extend down from the surface, the cast is free-fall, and the dot-dashed line indicates the free-rise up from the seafloor. For site 1, the dashed line indicates a second downcast, some 2.5 hr after the first downcast.

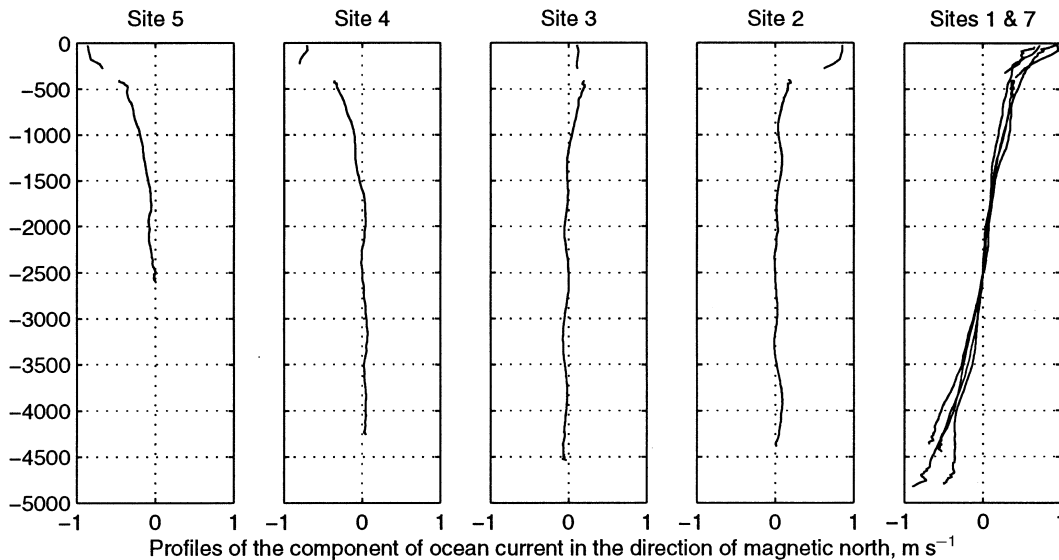


**Figure 12.** The profiler velocity data tied to zero at depth 2500m, with ship's ADCP profiles in the upper several hundred metres of the ocean column. For sites 1 and 7, two (consecutive) downcasts are plotted for site 1, and both the free-fall and the free-rise profiles are plotted for site 7, these latter extending down from the sea surface. The lower half of the profiles for sites 1 and 7 are considered to be influenced by seafloor magnetization effects, and should be ignored from an oceanographic point of view.

thus an excellent natural laboratory for studying motional induction in seawater.

## 7 CONCLUSIONS

It has been demonstrated that modern instrumentation has made the measurement of the total magnetic field down through the ocean column a straight-forward exercise. No more than standard magnetometer sensitivity is required to show, reflected in the magnetic profile, the profile of oceanic transport in the magnetic meridian. However, care needs to be taken regarding crustal magnetization effects, and time-fluctuation magnetic effects. The purpose of the 1997 SODA experiment was to seek an ocean velocity field with contrasting southwards and northwards flowing limbs, and to check in those limbs for magnetic effects predicted to be of opposite sign. This test appears to have been successful.

The vertical-profiling method demonstrated has an important dependence on the ambient magnetic inclination, and may be expected to work best in magnetic mid-latitudes. The method depends on magnetic inclination being neither vertical (as at the magnetic dip poles) nor horizontal (as at the magnetic equator). For a vertical inclination, the component of the horizontal perturbation field which is resolved into the total-field direction will be zero. For a horizontal inclination, the horizontal  $vB$  electric term in eq. (1) will be zero.

Thus it may be concluded that, against the background of a uniform gradient which reflects the origin of the main magnetic field in Earth's core, a vertical magnetic profile in the ocean will show perturbation fields due to crustal magnetization, induction from external source fields, and signals due to the motional induction by ocean currents. Within the limits stated above, the latter may be strong enough to stand out clearly, so that an observed total-field vertical profile, with quite minimal data reduction, may be inverted directly to give a profile, with depth, of the local ocean current velocity, resolved in the magnetic meridian.

The motional induction magnetic fields treated in this paper have the fundamental characteristic that they are not seen outside the ocean. In this they resemble the toroidal fields of Earth's main dynamo, which are not seen outside Earth's core.

## ACKNOWLEDGMENTS

The observations described have generally been made from the vessel RV Franklin, which in 1997 devoted ten days of ship time to the SODA experiment, of which this paper reports a major part. We are grateful for the support provided by this national research facility and for the contributions to our measurements made by her crew. Land data have been provided by the AGSO Canberra Magnetic Observatory, and the CICADA project, run particularly by Adrian Hitchman and Peter Milligan. AW and GSH acknowledge financial support from the Australian Research Council. Particular acknowledgement in this paper is made to the late Stanley Keith Runcorn. Prior to his untimely death at the end of 1995, his interest and encouragement in the present work earlier that year was given generously at an important time. As a key participant in the 1940s measurements of the vertical gradients of Earth's magnetic field, he drew the attention of the authors to the paper by Espersen *et al.* (1956). The authors have also benefitted from discussions with both Anton Hales (in Canberra) and Ian Gough (in Canada), the principal investigators in the South African mine measurements of the late 1940's. The interest and contributions of a range of oceanographers has also been important and appreciated. Peter Holloway was chief scientist of cruise Fr04/95. George Cresswell helped during the 1997 SODA experiment in interpreting satellite images of the EAC. Students Nathaniel Jewell, Andrew Kiss, David Robinson and Alan Wong helped at sea during Fr08/97. Generally conversations at different times with Nathan Bindoff, Alan Chave, Steve Constable, Nigel Edwards, Ian Ferguson, Augusta Flosadottir, Jean Filloux, Jim Larsen, Lawrie Law, Doug Luther, Phil Mulhearn, Paul Roberts, Tom Sanford, Hiroaki

Toh, Rob Tyler, Denis Winch and others have been most beneficial. Two referees suggested valuable improvements to the manuscript. Finally TL and AW acknowledge the lasting stimulation of the tearoom at Madingley Rise, Cambridge, some 35 years ago, when Edward Bullard instructed one of us (TL) in the matter of motional induction, and another of us (AW) in the matter of marine magnetometers. We are very happy to bring these two strands together in this paper, especially with the third author, now our colleague of more than ten years standing.

## REFERENCES

- Baines, P.G. & Bell, R.C., 1987. The relationship between ocean current transports and electric potential differences across the Tasman Sea, measured using an ocean cable, *Deep-Sea Res.*, **34**, 531–546.
- Barracough, D.R., *et al.*, 1992. 150 years of magnetic observatories: recent researches on world data, *Surv. Geophys.*, **13**, 47–88.
- Barton, C.E., 1997. International Geomagnetic Reference Field: the seventh generation, *J. Geomagn. Geoelectr.*, **49**, 123–148.
- Bindoff, N.L., 1988. Electromagnetic induction by oceanic sources in the Tasman Sea, *PhD thesis*, The Australian National University, Canberra.
- Bindoff, N.L., Filloux, J.H., Mulhearn, P.J., Lilley, F.E.M. & Ferguson, I.J., 1986. Vertical electric field fluctuations at the floor of the Tasman Abyssal Plain, *Deep-Sea Res.*, **33**, 587–600.
- Blackett, P.M.S., 1947. The magnetic field of massively rotating bodies, *Nature*, **159**, 658–666.
- Blackett, P.M.S., 1952. A negative experiment relating a magnetism and Earth's rotation, *Phil. Trans. R. Soc. Lond., A*, **245**, 309–370.
- Bullard, E.C., 1949. The magnetic field within the Earth, *Proc. R. Soc. London Ser. A*, **197**, 433–453.
- Burrows, K. & Hall, S.H., 1965. Rocket measurements of the geomagnetic field above Woomera, South Australia, *J. geophys. Res.*, **70**, 2149–2158.
- Chapman, S. & Runcorn, S.K., 1948. Variation of geomagnetic intensity with depth, *Nature*, **161**, 52.
- Chave, A.D. & Luther, D.S., 1990. Low-frequency, motionally-induced electromagnetic fields in the ocean: 1. theory, *J. geophys. Res.*, **95**, 7185–7200.
- Chave, A.D., Luther, D.S. & Filloux, J.H., 1997. Observations of the boundary current system at 26.5 degrees N in the subtropical North Atlantic ocean, *J. Phys. Oceanogr.*, **27**, 1827–1848.
- Cresswell, G.R. & Legeckis, R., 1986. Eddies off southeastern Australia, *Deep-Sea Res.*, **33**, 1527–1562.
- Espersen, J., Andreasen, P., Egedal, J. & Olsen, J., 1956. Measurements at sea of the vertical gradient of the main geomagnetic field during the Galathea Expedition, *J. geophys. Res.*, **61**, 593–624.
- Faraday, M., 1832. Experimental researches in electricity (Bakerian lecture), *Phil. Trans. R. Soc. Lond., A*, **122**, 163–194.
- Filloux, J.H., 1987. Instrumentation and experimental methods for oceanic studies, in *Geomagnetism*, pp. 143–247, ed Jacobs, J.A., Academic Press Inc, London.
- Flosadottir, A.H., Larsen, J.C. & Smith, J.T., 1997a. The relation of seafloor voltages to ocean transports in North Atlantic circulation models: Model results and practical considerations for transport monitoring, *J. Phys. Oceanogr.*, **27**, 1547–1565.
- Flosadottir, A.H., Larsen, J.C. & Smith, J.T., 1997b. Motional induction in North Atlantic circulation models, *J. geophys. Res.*, **102**, 10 353–10 372.
- Fujii, I. & Chave, A.D., 1999. Motional induction effect on the planetary-scale geoelectric potential in the eastern North Pacific, *J. geophys. Res.*, **104**, 1343–1359.
- Hales, A.L. & Gough, D.I., 1947. Blackett's fundamental theory of the Earth's magnetic field, *Nature*, **160**, 746.
- Heirtzler, J., 1967. Measurement of the vertical geomagnetic field gradient beneath the surface of the Arctic Ocean, *Geophys. Prospect.*, **15**, 194–203.
- Hide, R., 1997. Hide receives the Bowie Medal: Response, *EOS, Trans. Am. geophys. Un.*, **78**, 295–296.
- Hitchman, A.P., Lilley, F.E.M. & Campbell, W.H., 1998. The quiet daily variation in the total magnetic field: global curves, *Geophys. Res. Lett.*, **25**, 2007–2010.
- Hitchman, A.P., Lilley, F.E.M. & Milligan, P.R., 2000. Induction arrows from offshore floating magnetometers using land reference data, *Geophys. J. Int.*, **140**, 442–452.
- Lanzerotti, L.J., Chave, A.D., Sayres, C.H., Medford, L.V. & MacLennan, C.G., 1993. Large scale electric field measurements on the Earth's surface: A review, *J. geophys. Res.*, **98**, 23 525–23 534.
- Larsen, J.C., 1992. Transport and heat flux of the Florida Current at 27 deg N derived from cross-stream voltages and profiling data: theory and observations, *Phil. Trans. R. Soc. Lond., A*, **338**, 169–236.
- Lilley, F.E.M., Filloux, J.H., Bindoff, N.L., Ferguson, I.J. & Mulhearn, P.J., 1986. Barotropic flow of a warm-core ring from seafloor electric measurements, *J. geophys. Res.*, **91**, 12 979–12 984.
- Lilley, F.E.M., Filloux, J.H., Mulhearn, P.J. & Ferguson, I.J., 1993. Magnetic signals from an ocean eddy, *J. Geomagn. Geoelectr.*, **45**, 403–422.
- Longuet-Higgins, M.S., Stern, M.E. & Stommel, H., 1954. The electric field induced by ocean currents and waves, with applications to the method of towed electrodes, *Pap. Phys. Oceanogr. Meteorol.*, **13**, 1–37.
- Luther, D.S., Filloux, J.H. & Luther, D.S., 1991. Low-frequency, motionally-induced electromagnetic fields in the ocean: 2. Electric field and Eulerian current comparison, *J. geophys. Res.*, **96**, 12 797–12 814.
- Matsushita, S., 1967. Solar quiet and lunar daily variation fields, in *Physics of Geomagnetic Phenomena*, pp. 302–424, eds Matsushita, S. & Campbell, W.H., Academic Press Inc, New York.
- McElhinny, M.W. & McFadden, P.L., 2000. *Paleomagnetism: Continents and Oceans*, Academic Press Inc, San Diego.
- Merrill, R.T., McElhinny, M.W. & McFadden, P.L., 1996. *The Magnetic Field of the Earth: Paleomagnetism, the Core, and the Deep Mantle*, Academic Press Inc, San Diego.
- Palshin, N.A., 1996. Oceanic electromagnetic studies: a review, *Surv. Geophys.*, **17**, 455–491.
- Runcorn, S.K., 1948. The radial variation of the Earth's magnetic field, with an appendix by S. Chapman, *Proc. Phys. Soc.*, **61**, 373–382.
- Runcorn, S.K., Benson, A.C., Moore, A.F. & Griffiths, D.H., 1951. Measurements of the variation with depth of the main geomagnetic field, *Phil. Trans. R. Soc. Lond., A*, **244**, 113–151.
- Sanford, T.B., 1971. Motionally induced electric and magnetic fields in the sea, *J. geophys. Res.*, **76**, 3476–3492.
- Sanford, T.B., Drever, R.G. & Dunlap, J.H., 1985. An acoustic Doppler and electromagnetic velocity profiler, *J. Atmos. Ocean. Technol.*, **2**, 110–124.
- Stephenson, D. & Bryan, K., 1992. Large-scale electric and magnetic fields generated by the oceans, *J. geophys. Res.*, **97**, 15 467–15 480.
- Toh, H., Goto, T. & Hamano, Y., 1998. A new seafloor electromagnetic station with an Overhauser magnetometer, a magnetotelluric variograph and an acoustic telemetry modem, *Earth, Planet. Space*, **50**, 895–903.
- Tomczak, M. & Godfrey, J.S., 1994. *Regional Oceanography: An Introduction*, Pergamon Press, Oxford.
- Tyler, R.H., Sanford, T.B. & Oberhuber, J.M., 1997. Geophysical challenges in using large-scale ocean-generated EM fields to determine the ocean flow, *J. Geomagn. Geoelectr.*, **49**, 1351–1372.